

Automated Detection of Cancer Cells in Effusion Specimens by DNA Karyometry

Alfred H. Böcking, MD^{1,2,*}; David Friedrich, PhD^{3,7}; Dietrich Meyer-Ebrecht, PhD³;
Chenyan Zhu, PhD⁴; Anna Feider, MD⁵; and Stefan Biesterfeld, MD⁶

BACKGROUND: The average sensitivity of conventional cytology for the identification of cancer cells in effusion specimens is only approximately 58%. DNA image cytometry (DNA-ICM), which exploits the DNA content of morphologically suspicious nuclei measured on digital images, has a sensitivity of up to 91% for the detection of cancer cells. However, when performed manually, to our knowledge to date, an expert needs approximately 60 minutes for the analysis of a single slide. **METHODS:** In the current study, the authors present a novel method of supervised machine learning for the automated identification of morphologically suspicious mesothelial and epithelial nuclei in Feulgen-stained effusion specimens. The authors compared this with manual DNA-ICM and a gold standard cytological diagnosis for 121 cases. Furthermore, the authors retrospectively analyzed whether the amount of morphometrically abnormal mesothelial or epithelial nuclei detected by the digital classifier could be used as an additional diagnostic marker. **RESULTS:** The presented semiautomated DNA karyometric solution identified more diagnostically relevant abnormal nuclei compared with manual DNA-ICM, which led to a higher sensitivity (76.4% vs 68.5%) at a specificity of 100%. The ratio between digitally abnormal and all mesothelial nuclei was found to identify cancer cell-positive slides at 100% sensitivity and 70% specificity. The time effort for an expert therefore is reduced to the verification of a few nuclei with exceeding DNA content, which to our knowledge can be accomplished within 5 minutes. **CONCLUSIONS:** The authors have created and validated a computer-assisted bimodal karyometric approach for which both nuclear morphology and DNA are quantified from a Feulgen-stained slide. DNA karyometry thus increases the diagnostic accuracy and reduces the workload of an expert when compared with manual DNA-ICM. *Cancer Cytopathol* 2019;127:18-25. © 2018 The Authors. *Cancer Cytopathology* published by Wiley Periodicals, Inc. on behalf of American Cancer Society. This is an open access article under the terms of the Creative Commons Attribution-NonCommercial-NoDerivs License, which permits use and distribution in any medium, provided the original work is properly cited, the use is non-commercial and no modifications or adaptations are made.

KEY WORDS: automated cytology; DNA cytometry; DNA image cytometry; DNA karyometry; nuclear classifiers; serous effusions.

INTRODUCTION

Body cavity effusion specimens of unknown etiology need to be investigated cytologically. In approximately 40% of effusions, metastasizing malignant tumors or mesotheliomas are the cause.¹ The microscopic screening of smears from effusion sediments is time-consuming and requires skilled personnel. The sensitivity is only approximately 58%, and the specificity is approximately 97.0% on average.² Interobserver reproducibility reveals a kappa value of only 0.514.³

Numerous adjuvant methods have been proposed to increase the diagnostic accuracy of effusion specimens, such as immunocytochemistry, applying different markers (sensitivity of 82.2% and specificity of 100%),^{4,5} fluorescence in situ hybridization targeted toward various chromosomal aneuploidies (sensitivity of 79% and specificity of 100%),⁶ quantitative methylation-specific polymerase chain

Corresponding author: Alfred Hermann Böcking, MD, Heidenheimer Strasse 6, 13467 Berlin, Germany; Alfred.boecking@web.de

¹Institute of Cytopathology, University of Dusseldorf, Dusseldorf, Germany; ²Department of Cytopathology, City Hospital Duren, Duren, Germany; ³Institute of Image Analysis and Computer Vision, RWTH Aachen University, Aachen, Germany; ⁴Motic Medical Diagnostic Systems Company LTD, Xiamen, China; ⁵Praxis Dr. Link, Mettmann, Germany; ⁶Institute of Pathology, Koblenz, Germany; ⁷Definiens AG, Munich, Germany

Received: June 12, 2018; **Revised:** August 12, 2018; **Accepted:** September 6, 2018

Published online October 19, 2018 in Wiley Online Library (wileyonlinelibrary.com)

DOI: 10.1002/cncy.22072, wileyonlinelibrary.com

reaction (sensitivity of 49.4% and specificity of 98.4%),⁷ argyrophilic nucleolar organizer regions (AgNORs; sensitivity of 97.5% and specificity of 100%),⁸ and DNA image cytometry (DNA-ICM; sensitivity of 75.0% and specificity of 100%).⁹ Combining several biomarkers with cytomorphology reportedly can increase sensitivity.^{5,7}

A method that also can be used for the primary screening of effusion sediments is DNA cytometry. It measures overall nuclear DNA content in Feulgen-stained specimens as a diagnostic marker and analyzes their distribution (DNA ploidy analysis). The cytometric equivalence of chromosomal aneuploidy, called DNA aneuploidy (stemline and single cell) is used as a specific marker for malignancy.¹⁰ DNA flow cytometry does not differentiate between different cell types, and thus often misses minor cell populations such as a few cancer cells in a majority of reactive mesothelial and inflammatory cells.⁹ Instead, because the objective of DNA-ICM is the specific measurement of morphologically abnormal nuclei, it reaches higher sensitivities. As a quantitative method, DNA-ICM demonstrates a nearly perfect reproducibility, with a kappa of 0.87 in cervical brush biopsies.¹¹ Unfortunately, the manual measurement of some hundred nuclei takes on average between 40 and 60 minutes. To the best of our knowledge, approaches for computer-assisted DNA-ICM using scanning microscopes have not yet allowed for the differentiation of nuclei from different cell types, nor between normal and abnormal cells.^{12–15}

In the current study, we have presented and evaluated a novel solution for rapid, computer-assisted, semi-automated diagnostic DNA cytometry of serous effusion specimens: DNA karyometry (DNA-KM). We define it as a combination of automated morphometric, cell type-specific classification of nuclei with image cytometric measurement of their DNA content. Its core component is a machine learning algorithm that distinguishes between morphologically normal and abnormal nuclei from different cell types and artifacts in Feulgen-stained smears. DNA measurements then can be performed in a cell type-specific way. We also compare the diagnostic accuracy of manual DNA-ICM and automated DNA-KM, and the separate use of morphometric features are examined as an additional diagnostic marker with which to increase sensitivity.

MATERIALS AND METHODS

Specimens

In 2012, a total of 136 consecutive serous effusion specimens were selected from probes and routinely sent to the department of cytopathology at the Institute of Pathology of the University Clinics in Düsseldorf, Germany, for cytological diagnostic evaluation. A total of 87 were pleural effusions, 3 were pericardial effusions, and 37 were peritoneal effusions, and 9 cases were intraoperative washings of the peritoneal cavity. A total of 6 smears per probe were prepared routinely after centrifugation, 3 of which were air dried and stained according to the May-Grunwald-Giemsa method and 3 of which were fixed with alcoholic spray and stained according to the Papanicolaou method. Primary cytological diagnoses were obtained on these 6 slides by one of the authors (S.B.). One additional May-Grunwald-Giemsa-stained slide was prepared for a postponed second-opinion diagnosis by one of the authors in Aachen (A.B.), and another air-dried slide was used for Feulgen staining.^{16,17} A total of 15 smears had to be excluded because of a paucity of cells in the additionally prepared slide (<30 lymphocytes and/or <300 mesothelial cells). Thus, 121 specimens remained for DNA-KM, comprising 77 pleural effusions, 3 pericardial effusions, 36 peritoneal effusions, and 5 intraoperative washings of the peritoneal cavity.¹⁸

Cytology and Clinical Follow-Up

The primary cytological diagnoses were made as follows: 59 specimens were without malignant cells, 14 specimens were suspicious for malignant cells, and 48 specimens were found to have malignant cells. To establish a gold-standard final diagnosis, subsequent immunocytochemical tests using BerEP4 and human epithelial antigen as epithelial markers were performed on the 14 suspicious specimens. Detection of immunoreactive cells was taken as evidence of metastatic cancer cells (10 specimens). In addition, in these 14 cases, clinicians were contacted by mail concerning the clinical proof of metastatic cancers. This was confirmed in 10 of these cases. Thus, the basic “truth” consisted of: 1) 58 cases without tumor cells as verified by 2 pathologists; 2) 4 cases without tumor cells as verified by 2 pathologists and by immunocytochemistry; 3) 10 cases with tumor cells noted by immunocytochemistry and clinical follow-up; and 4) 49 cases with tumor cells as verified by 2 pathologists.

Primary cytological diagnoses of “suspicious for malignant cells” were assessed as “positive for malignant cells” when calculating diagnostic accuracy.

Feulgen Staining

Hydrolysis was applied in 5N of hydrochloric acid at 20°C for 60 minutes, using a temperature-controlled cuvette and a Varistain 24-3 staining machine (Thermo Shandon Ltd, Runcorn, United Kingdom).¹⁹ Schiff reagent was used (Nr. 1.09033.0500; Merck, Darmstadt, Germany).

Approximately 2 cm × 2 cm regions containing sufficient cells were marked for DNA cytometry and DNA-KM, respectively, with felt tip pen on each slide. All Feulgen-stained slides were processed by manual DNA cytometry as well by automated DNA-KM.

Manual DNA-ICM

For manual DNA cytometry, a MotiCyte DNA manual system (V1.0; Motic China Group Ltd, Xiamen, China) was used. It consists of a Motic BA 410 microscope with a ×40 objective, a working distance of 0.5 mm, a condenser numerical aperture (NA) of 0.65 and a camera adapter of factor 0.87, a charge-coupled device camera (scientific grade MotiCam Pro 285A; Motic China Group Ltd), and a PC with a high-resolution monitor. Kohler illumination was applied before each measurement. A black-and-white image balance was performed before each measurement. Nuclei were selected at random per mouse click on the monitor by one of the authors (A.F.). At least 30 lymphocytes were chosen as internal reference cells. Their coefficient of variation to be <5%.²⁰ Their mean integrated optical density (IOD) value was defined as 2c per slide. In slides without cytological suspicion of malignant cells, nuclei from normal mesothelial cells were chosen as analysis cells. In smears that were suspicious for or with evidence of malignant cells, their nuclei were chosen as analysis cells. All nuclear images were stored in an image gallery for optional later control or reclassification as necessary. The resulting cell type-specific nuclear DNA contents were presented in histograms (number of cells vs DNA content in cell) (Figs. 1 and 2).

Automated DNA-KM Measurements

A motorized Motic BA 610 microscope (Motic China Group Ltd) was used with a ×40 objective (NA of 0.65) and a MotiCam CCD camera 285A was used with 1360 × 1024 pixel resolution. The software used was MotiCyte

screeener 2.3 (Motic China Group Ltd) with a digital nuclear classifier for effusion specimens.²¹ The classifier had been trained on Feulgen-stained slides from effusion sediments to automatically discriminate nuclei from normal mesothelial cells, atypical and abnormal mesothelial cells suspicious of or proving malignancy, macrophages, lymphocytes, granulocytes, defocused nuclei, and artifacts.

Screening was restricted to the marked areas and took between 40 and 60 minutes per slide. All objects automatically classified as artifacts or defocused nuclei >9c finally had been reassessed and reclassified if necessary on the image gallery by an experienced cytopathologist (A.B.). This took approximately 5 minutes per slide.

Machine Learning Approach

The digital nuclear classifier for karyometry was trained on an annotated database of images from 54,374 Feulgen-stained nuclei derived from 9 different slides of serous effusions (gold standard). The primary subjective classification of nuclei was performed by an experienced cytopathologist (A.B.). A total of 18 different morphometric features were used, 11 of which described the morphology of nuclei, 4 of which were pixel values of the brightfield images, and 3 of which were textural information regarding nuclei. A description of these features and the rationale for choosing them can be found in Table 1. The random forest classifier²² was applied. For other tumor indications, this classifier performed in a manner comparable to that of support vector machines and outperformed k nearest neighbor classifiers, conventional decision trees, neural networks, or the AdaBoost classifier.²¹ Approximately 95.2% of abnormal nuclei were correctly identified by the classifier, and 2.9% of artifacts were misclassified as abnormal. Approximately 3.5% of abnormal nuclei had been classified erroneously as artifacts, and 4.2% of objects that automatically were classified as artifacts were abnormal nuclei.²¹

Diagnostic Interpretation

DNA stemlines were identified automatically in histograms as distinct peaks with additional values at their doubling position according to Haroske et al.²³

DNA stemline aneuploidy was assumed if the mean value of the nuclear DNA content of a stemline was >/<10% of 2c or 4c.²³ Single-cell DNA aneuploidy was assumed if >3 nuclei of >9c occurred (9c exceeding events [9c EE])

TABLE 1. Description of the Features Used for Analysis

| Feature | Description |
|-------------------|---|
| Area | Area of the segmentation mask |
| Perimeter | Perimeter of the segmentation mask |
| MinRadius | Smallest distance from the centroid to the contour |
| MaxRadius | Largest distance from the centroid to the contour |
| MeanRadius | Average distance from the centroid to the contour |
| VarianceRadius | Variance of the distances from the centroid to the contour |
| Sphericity | Fraction of MinRadius and MaxRadius |
| Eccentricity | Ratio of the major to minor axis of the best-fit ellipse |
| Inertia | Squared distance of all the object's pixels to the centroid, normalized by the squared area |
| Compactness | $P^2/(4\pi A)$, in which P is the perimeter and A is the area |
| BendingEnergy | Energy needed to bend the contour to its current shape |
| Background | Average intensity of all pixel values >150 in a small reference region around the nucleus |
| MeanLuminance | Average intensity of the gray image |
| VarLuminance | Variance of intensity values of the gray image |
| MinFilter | Minimum response of a square filter on the gray image |
| Entropy | Entropy of the gray image |
| ClusterShade | Contrast between dark clumps and light background |
| ClusterProminence | "Darkness" of clusters |

Abbreviations: Max, maximum; Min, minimum; Var, variance.

To test the ability of digital nuclear classifiers to increase the diagnostic sensitivity of DNA-KM for the detection of malignant nuclei, a ratio between digitally abnormal and all mesothelial nuclei of ≥ 0.75 was found to be a diagnostically useful threshold. Cases with a lower percentage of abnormal nuclei would be classified as "without malignant cells."

Statistical Analysis

SPSS statistical software (version 22.0.001; IBM Corporation, Armonk, New York) was used.

The current study was approved by the ethics committee of Heinrich Heine University in Dusseldorf (study number 4064).

RESULTS

The mean number of lymphocytes automatically identified per slide by digital nuclear classifiers was approximately 100 times higher than the number selected manually (3734.1 vs 33.8) (Table 2). The number of

TABLE 2. Number of Reference and Analysis Cells Measured per Slide

| Type of Measurement | Manual | Auto | Manual | Auto |
|---------------------|-----------------|--------|----------------|-------|
| | Reference Cells | | Analysis Cells | |
| Mean value | 33.8 | 3734.1 | 235.4 | 302.6 |
| SD | 5.0 | 4846.5 | 85.3 | 866.3 |
| Maximum value | 50 | 32106 | 472 | 7942 |

Abbreviations: Auto, automatic; SD, standard deviation.

TABLE 3. Number of 9c Exceeding Events and DNA Stemlines Detected per Slide

| Value | Manual | Auto | Manual | Auto |
|---------------|--------|------|---------------------|------|
| | 9c EEs | | Aneuploid Stemlines | |
| Mean value | 2.0 | 3.6 | 0.44 | 0.37 |
| SD | 6.2 | 15.4 | 0.77 | 0.69 |
| Maximum value | 36 | 137 | 3 | 3 |

Abbreviations: 9c EE, 9c exceeding events; Auto, automatic; SD, standard deviation.

morphologically abnormal or atypical nuclei per slide detected by DNA-KM exceeded that of manual selection by a mean of 67 (302.6 vs 235.4) (Table 2). As a consequence, the mean number of 9c EEs found by DNA-KM exceeded that of manual selection by 1.6 times (Table 3). The maximum number of detected aneuploid DNA stemlines was 3 for both DNA-KM and manual selection (Table 3).

The time effort required for the subjective verification of a correct digital classification of objects per slide on the image gallery related to artifacts >9c possibly misclassified as abnormal nuclei ($\bar{x} = 165.6$) and to abnormal nuclei possibly misclassified as artifacts ($\bar{x} = 3.38$) was approximately 5 minutes (Figs. 1 and 2). One artifact in every seventh slide was misclassified as abnormal and 2 abnormal nuclei per every 3 slides were misclassified as artifacts. The time needed for control per slide was approximately 5 minutes.

Due to a greater representation of nuclear sampling, semiautomated DNA-KM correctly identified 4 more slides with cancer cells compared with subjective DNA-ICM, without causing false-positive diagnoses. Thus, the diagnostic sensitivity of this method exceeded that of manual cytometry by approximately 8% without any decrease in specificity noted (Tables 4 and 5).

Using the percentage of morphometrically abnormal nuclei relative to all normal mesothelial nuclei, $\geq 0.75\%$ evolved as a sufficiently sensitive threshold with

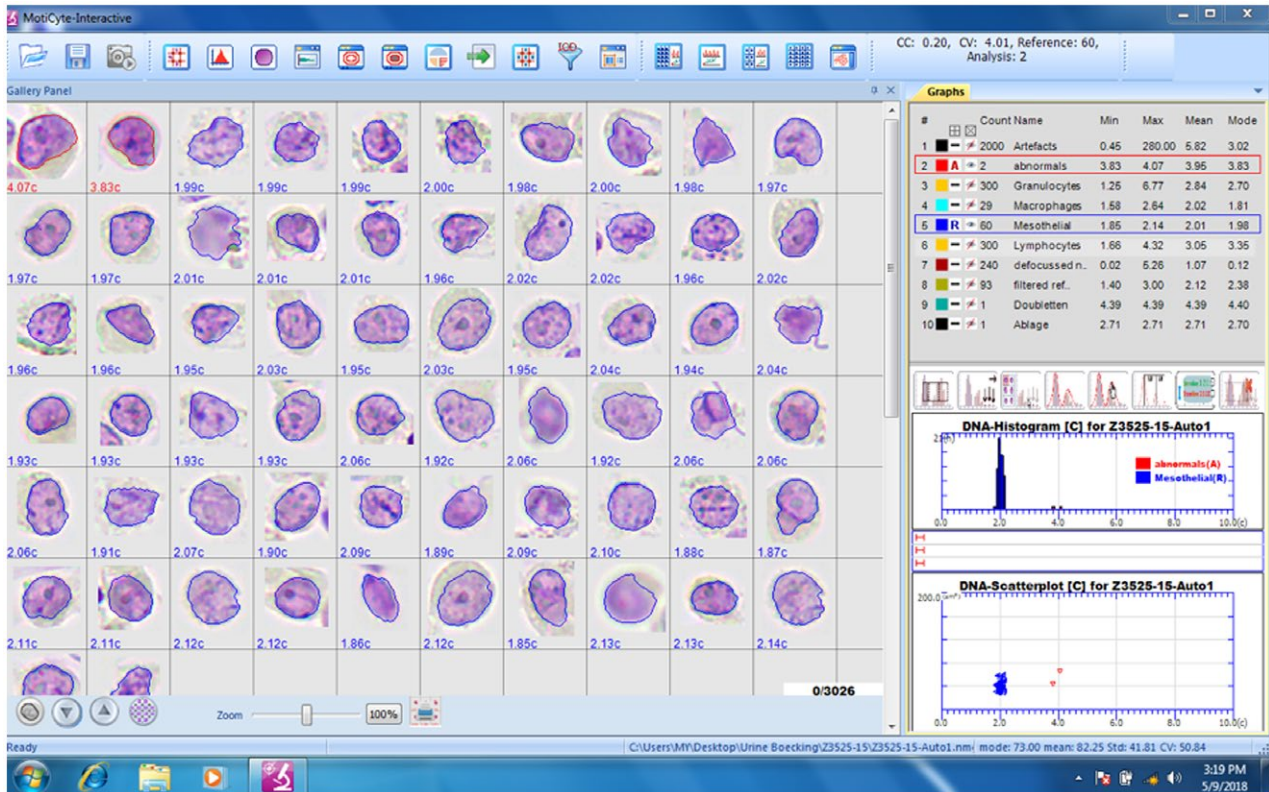


Figure 1. Screenshot from a monitor of a MotiCyte-auto, demonstrating 60 images of automatically classified, Feulgen-stained nuclei of regular mesothelial cells as the internal reference and 2 abnormal nuclei from a serous effusion specimen without malignant cells. (Top Right) Data regarding measured nuclei. (Bottom Right) DNA histogram (DNA content vs number) demonstrating DNA diploidy of mesothelial cells and a scatterplot (area vs number) of measured normal mesothelial and abnormal nuclei. Max indicates maximum; min, minimum.

which to identify all slides containing malignant cells, at a specificity of 70% (Table 4).

DISCUSSION

In the current study, we have established and validated a bimodal, semiautomated cytometric procedure for the detection of cancer cells (DNA-KM) in effusion specimens based on the digital nuclear classification of nuclei according to cell type and nuclear DNA content. Semiautomated DNA-KM appears to increase diagnostic accuracy compared with screening of smears from effusion sediments, frees the time of highly trained personnel for performing additional tasks, and enables the use of the percentage of abnormal nuclei as a new diagnostic (screening) marker.

In most countries of the world, there are not sufficient numbers of well-trained cytotechnicians and cytopathologists available to screen slides for cancer cells from serous effusion sediment specimens. In addition, the manual procedure is

time-consuming, and therefore a semiautomated procedure to improve diagnostic efficiency would be very useful.

First, digital nuclear classifiers had to be trained to automatically classify Feulgen-stained nuclei as different cell types (lymphocytes, granulocytes, macrophages, and artifacts). Second, morphologically atypical and abnormal nuclei had to be differentiated from normal or reactive mesothelial cells. Our intention in choosing 18 features, as described in Table 1, was to use predominantly morphological features as classification criteria because morphology is the key discriminator between 1) abnormal and normal mesothelial nuclei, and 2) abnormal nuclei and clustered/overlapping nuclei. The pixel values of the brightfield images are required to distinguish nuclei from artifacts with a clear difference, such as nuclei overlapping with dirt particles or glass splinters, which occasionally are segmented by the segmentation algorithm. Finally, the texture of a nucleus again is needed to quantify differences between normal and abnormal mesothelial nuclei.

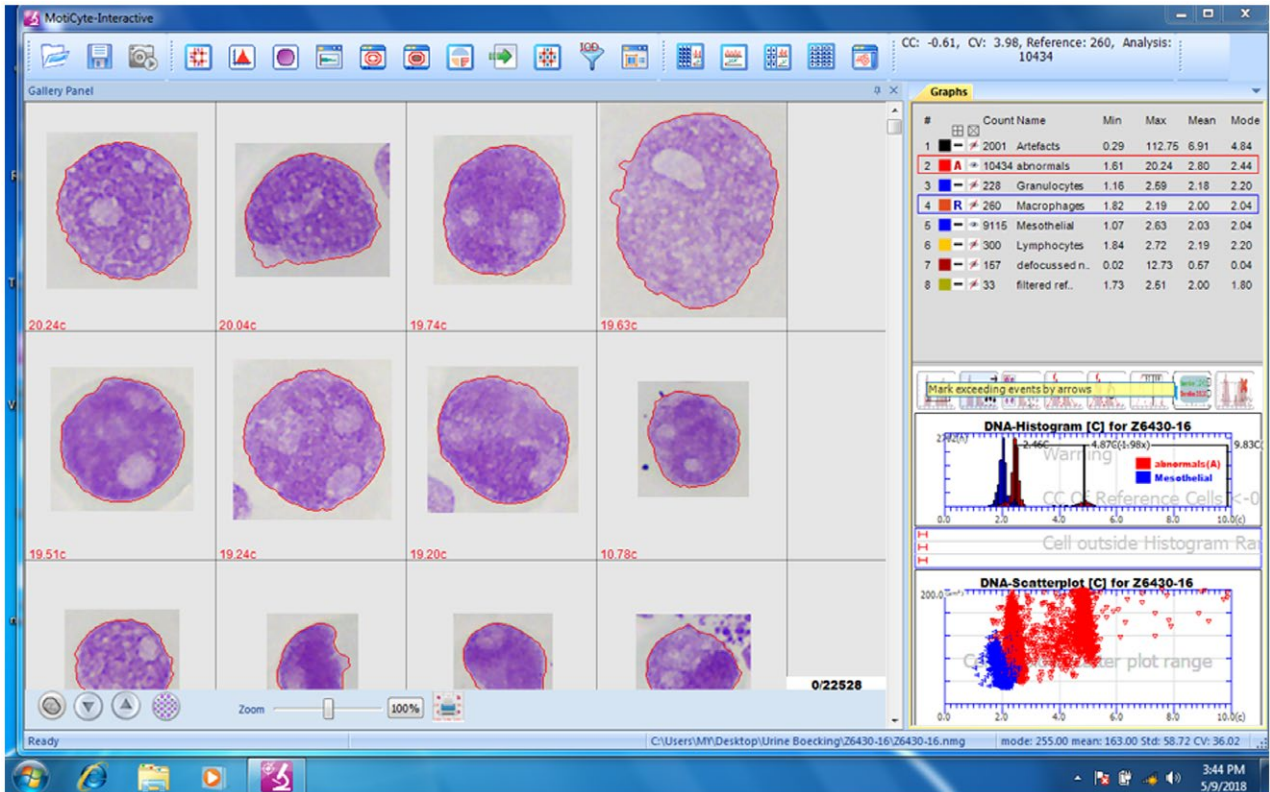


Figure 2. Screenshot from a monitor of a MotiCyte-auto demonstrating images of 12 automatically classified nuclei from Feulgen-stained, abnormal cells from a serous effusion specimen with cancer cells. (Top Right) Data regarding measured nuclei. (Bottom Right) DNA histogram (DNA content vs number) revealing DNA aneuploidy with DNA stemlines at 2.46c and 4.87c and a scatterplot (area vs number) of measured abnormal nuclei. Max indicates maximum; min, minimum.

TABLE 4. Four-Field Tables of Cytology, Manual DNA-ICM, Automated DNA-KM, and Automated M-KM

| Final Diagnosis | Cytology | | Manual DNA-ICM | | Automated DNA-KM | | Automated M-KM | |
|-----------------|----------|----------|----------------|----------|------------------|----------|----------------|----------|
| | Positive | Negative | Positive | Negative | Positive | Negative | Positive | Negative |
| Positive | 54 | 5 | 37 | 17 | 41 | 13 | 57 | 0 |
| Negative | 0 | 62 | 0 | 67 | 1 | 66 | 19 | 45 |

Abbreviations: DNA-ICM, manual DNA image cytometry; DNA-KM, DNA karyometry; M-KM, morphometric karyometry.

TABLE 5. Diagnostic Accuracy of Cytology, Manual DNA-ICM, Automated DNA-KM, and Automated M-KM

| | Cytology | Manual DNA-ICM | Automated DNA-KM | Automated M-KM |
|-------------|----------|----------------|------------------|----------------|
| Sensitivity | 88.5% | 68.5% | 76.4% | 100% |
| Specificity | 100% | 100% | 100% | 70% |
| PPV | 100% | 100% | 100% | 75% |
| NPV | 89.4% | 79.8% | 83.5% | 100% |

Abbreviations: DNA-ICM, manual DNA image cytometry; DNA-KM, DNA karyometry; M-KM, morphometric karyometry; NPV, negative predictive value; PPV, positive predictive value.

The correct nuclear classification rates were 87.1%, 81.5%, 41.3%, 88.4%, 95.2%, and 90.4%, respectively, for lymphocytes, granulocytes, macrophages, artifacts,

atypical or abnormal nuclei, and normal or reactive mesothelial cells. The poor results for macrophages may be explained by their morphologic heterogeneity. Overall,

the rate of correct nuclear classification was 88.1%.²¹ These classifications allowed cell type-specific nuclear DNA measurements.

The precision of nuclear DNA measurements using the MotiCyte DNA device and rat liver imprints according to the proposals of the European Society for Analytical Cellular Pathology (ESACP)²⁴ have been reported by Berger-Frohlig.²⁵ Measuring 96 liver imprints from 2 different rats and using 50 lymphocytes as internal reference cells, the mean *c*-value for diploid hepatocytes was 1.99, was 4.01 for tetraploid hepatocytes, and was 7.96 for octoploid hepatocytes. The mean cell volume for lymphocytes per imprint was 2.80%.

The development of digital diagnostic classifiers for Feulgen-stained nuclei was described for oral smears,²⁶ prostate cancer cells,²⁷ and serous effusion specimens.²¹ One of their aims was to specifically identify the nuclei of different cell types such as normal epithelial or mesothelial cells, fibroblasts, lymphocytes, granulocytes, macrophages, and artifacts, whereas the other objective was the specific identification of morphologically suspicious, atypical, or dyskaryotic epithelial nuclei (mesothelial nuclei [ie, that derived from dysplasias]) and of abnormal nuclei from malignant epithelial or mesothelial cells, which all are abnormal. The respective classifier was trained by one of the authors (A.B.) using 54,373 Feulgen-stained nuclei from 9 different effusion specimens with known diagnoses. DNA measurements to identify aneuploidy as a specific marker for malignancy focused on these. The advantage of this procedure is that DNA aneuploidy may be identified in a minority of abnormal cells, whereas a majority of diagnostically irrelevant nuclei (eg, those from lymphocytes, granulocytes, and macrophages) are neglected. Thus, the sensitivity to detect few aneuploid cells will increase.

Kayser et al²⁷ also reported on manual DNA-ICM in pleural effusion specimens from 294 cases. They achieved a sensitivity of 91% and a specificity of 100%. Nevertheless, approximately 40.8% of slides had been rejected because of a paucity of cells. The authors used a lower threshold for single-cell aneuploidy, $9c\ EE \geq 1$, as was applied in the current study ($9c\ EE \geq 3$).

The results of the current study demonstrate that this automated combined procedure of digital nuclear morphometric classification and precise nuclear DNA

measurement, named DNA-KM, yields an even higher diagnostic sensitivity (76.5%) compared with manual DNA-ICM (68.5%). To exclude rare nuclear misclassifications, a final subjective check of classification results on the image galleries of abnormal findings and of artifacts is mandatory.

This sensitivity for the semiautomated detection of malignant cells in serous effusion specimens appears to be higher than the mean reported in the literature (58%) for conventional cytological diagnostics without adjuvant methods.

Because the specificity of this semiautomated diagnostic approach is 100%, the detection of DNA aneuploidy in serous effusion specimens allows for the definite diagnosis of malignant cells. In cases in which no aneuploidy is detected but $\geq 0.75\%$ of abnormal nuclei are noted, a suspicion of the presence of abnormal cells could be raised. Nevertheless, this will lower the specificity to 70%. Additional subjective inspection of slides and adjuvant diagnostic methods thus could be restricted to the approximately 30% of slides with $\geq 0.75\%$ of morphologically suspicious cells.

The solution presented herein does not represent a “black box” because all steps of automated diagnostic assessment can be controlled by the user and corrected if necessary.

An average of 5 minutes of human interaction (but in any event, a maximum 10 minutes) are needed per slide, thus reducing the workload for screening human serous effusion specimens for cancer cells. The time needed for the machine to screen slides can be reduced by applying this technology to automated digital slide scanners.

In the future, the threshold of 0.75 to label a case as “suspicious” based on the ratio of cells classified as abnormal and all mesothelial cells should be validated on a separate test set.

FUNDING SUPPORT

A grant was provided by MotiC Inc to pay approximately 50% of the salary of a research assistant at the Institute of Imaging and Computer Vision in Aachen, Germany, for 2 years for the joint development of software.

CONFLICT OF INTEREST DISCLOSURES

Alfred Hermann Böcking has acted as a paid scientific advisor for MotiC Inc for work performed outside of the current study. Chenyan Zhu has received personal fees from MotiC Inc for work performed outside of the current study.

AUTHOR CONTRIBUTIONS

Alfred H. Böcking: Conceptualization, methodology, data curation, formal analysis, funding acquisition, writing—original draft, and writing—review and editing. **David Friedrich:** Conceptualization, methodology, data curation, formal analysis, and writing—review and editing. **Dietrich Meyer-Ebrecht:** Conceptualization, project administration, funding acquisition, and writing—review and editing. **Chenyan Zhu:** Methodology and writing—review and editing. **Anna Feider:** Data curation, formal analysis, and writing—review and editing. **Stefan Biesterfeld:** Conceptualization, project administration, methodology, data curation, formal analysis, and writing—review and editing.

REFERENCES

1. Bedrossian CWM. Malignant Effusions. A Multimodal Approach to Cytologic Diagnosis. New York: Igaku-Shoin Medical Publishers; 1994.
2. Spriggs AI, Boddington MM. Atlas of serous fluid cytopathology. A guide to the cells of pleural, pericardial, peritoneal and hydrocele fluids. In: Gresham GA, ed. Current Histopathology Series. Vol 14. Dordrecht, Germany: Kluwer Academic Publishers; 1989:1-10.
3. Fassina A, Fedeli U, Corradin M, Da Fre M, Fabbris L. Accuracy and reproducibility of pleural effusion cytology. *Leg Med (Tokyo)*. 2008;10:20-25.
4. Motherby H, Nadjari B, Friegel P, Kohaus J, Ramp U, Böcking A. Diagnostic accuracy of effusion cytology. *Diagn Cytopathol*. 1999;20:350-357.
5. Motherby H, Kube M, Friedrichs D, et al. Immunocytochemistry and DNA-image cytometry in diagnostic effusion cytology I. Prevalence of markers in tumour cell positive and negative smears. *Anal Cell Pathol*. 1999;19:7-20.
6. Savić S, Franco N, Grilli B, et al. Fluorescence in situ hybridization in the definitive diagnosis of malignant mesothelioma in effusion cytology. *Chest J*. 2010;138:137-144.
7. Schramm M, Wrobel C, Born I, et al. Equivocal cytology in lung cancer diagnosis: improvement of diagnostic accuracy using adjuvant multicolor FISH, DNA-image cytometry, and quantitative promoter hypermethylation analysis. *Cancer Cytopathol*. 2011;119:177-192.
8. Pomjanski N, Motherby H, Buckstegge B, Knops K, Rohn BL, Böcking A. Early diagnosis of mesothelioma in serous effusions using AgNOR analysis. *Anal Quant Cytol Histol*. 2001;23:151-160.
9. Motherby H, Pomjanski N, Kube M, et al. Diagnostic DNA-flow-vs. -image-cytometry in effusion cytology. *Anal Cell Pathol*. 2002;24:5-15.
10. Böcking A. Comparability of tumor-cytogenetics and DNA-cytometry. *Mol Cytogenet*. 2015;8:28.
11. Nguyen VQ, Grote HJ, Pomjanski N, Knops K, Böcking A. Interobserver reproducibility of DNA-image-cytometry in ASCUS or higher cervical cytology. *Cell Oncol*. 2004;26:143-150.
12. Ploem JS, Verwoerd N, Bonnet J, Koper G. An automated microscope for quantitative cytology combining television image analysis and stage scanning microphotometry. *J Histochem Cytochem*. 1979;27:136-143.
13. Cornelisse CJ, van Driel-Kulker AM, Meyer F, Ploem JS. Automated recognition of atypical nuclei in breast cancer cytology specimens by iterative image transformations. *J Microsc*. 1985;137(pt 1):101-110.
14. Palcic B, MacAulay C, Harrison S, et al, inventors. System and method for automatically detecting malignant cells and cells having malignancy-associated changes. US Patent 6,026,174. February 15, 2000.
15. Palcic B, Garner DM, Beveridge J, et al. Increase of sensitivity of sputum cytology using high-resolution image cytometry: field study results. *Cytometry*. 2002;50:168-176.
16. Feulgen R, Rossenbeck H. Mikroskopisch-chemischer Nachweis einer Nukleinsäure vom Typus der Thymonukleinsäure und die darauf beruhende elective Färbung von Zellkernen in mikroskopischen Präparaten. *Hoppe-Seyler's Z Physiol Chem*. 1924;135:203-248.
17. Kasten F. Cytophotometric investigations of the influence of fixation on Feulgen hydrolysis: evidence for random loss of purines and pyrimidines from DNA during acid hydrolysis. *Acta Histochem Suppl*. 1971;9:637-647.
18. Feider A. Testing an automated DNA-cytometric device on air-dried effusion-specimens [medical dissertation]. *Duesseldorf, Germany: University of Dusseldorf*. 2018.
19. Chatelain R, Willms A, Biesterfeld S, Auffermann W, Böcking A. Automated Feulgen staining with a temperature-controlled staining machine. *Anal Quant Cytol Histol*. 1989;11:211-217.
20. Haroske G, Giroud F, Reith A, Böcking A. 1997 ESACP consensus report on diagnostic DNA image cytometry. Part I: basic considerations and recommendations for preparation, measurement and interpretation. European Society for Analytical Cellular Pathology. *Anal Cell Pathol*. 1998;17:189-200.
21. Friedrich D. Effective improvement of cancer diagnostics and prognostics by computer-assisted cell image analysis [PhD thesis]. Aachen, Germany: RWTH Aachen University; 2015.
22. Breiman L. Random forests. *Mach Learn*. 2001;45:5-32.
23. Haroske G, Baak JP, Danielsen H, et al. Fourth updated ESACP consensus report on diagnostic DNA image cytometry. *Anal Cell Pathol*. 2001;23:89-95.
24. Giroud F, Haroske G, Reith A, Böcking A. 1997 ESACP consensus report on diagnostic DNA image cytometry. Part II: specific recommendations for quality assurance. European Society for Analytical Cellular Pathology. *Anal Cell Pathol*. 1998;17:201-208.
25. Berger-Frohlig B. Improvement the precision of measurement of diagnostic DNA-image-cytometry. [MD thesis]. Dusseldorf, Germany: University of Dusseldorf; 2018.
26. Böcking A, Friedrich D, Jin C, et al. Diagnostic cytometry. In: Mehrotra D, ed. Oral Cytology. A Concise Guide. Berlin: Springer; 2013:125-146.
27. Kayser K, Blum S, Beyer M, Haroske G, Kunze KD, Meyer W. Routine DNA cytometry of benign and malignant pleural effusions by means of the remote quantitation server Euroquant: a prospective study. *J Clin Pathol*. 2000;53:760-764.